Chalcogenide Letters Vol. 14, No. 8, August 2017, p. 357 - 363

ANALYSIS ON ENERGY BANDGAP OF ZINC SULPHIDE (ZnS) THIN FILMS GROWN BY SOLUTION GROWTH TECHNIQUE

P. E. AGBO[a.b], P. A. NWOFE[b*], L. O. ODO[b,c]
[a]*Department of Physics/Geophysics and Geology, Faculty of Science, Federal University, Ndufu-Alike Ikwo, Nigeria*
[b]*Department of Industrial Physics, Faculty of Science, Ebonyi State University, Abakaliki, Nigeria*
[c]*Department of Physics, Federal College of Education, Eha-amufu, Nigeria*

Zinc sulphide thin films were grown on glass substrates using the solution growth technique. The films were grown at vary concentrations in the range 0.3 M to 0.7 M, with other deposition variables such as the bath temperature, pH, and deposition time were kept constant. The films were then subjected to post deposition annealing in order to improve on their crystallinity. Optical studies were obtained using UV- spectrophotometer. The effects of varying Zn^{2+} concentration and influence of annealing temperature on the optical properties of the deposited ZnS thin films were investigated with special emphasis on the tailoring of the bandgap. The optical parameters were found to vary with concentration of Zn^{2+} and post deposition annealing. Annealing slightly improved the bandgap of the films. The band gaps of all samples were in range of 3.50–3.76 eV. The values of the energy bandgap strongly indicate that the films will be used in different optoelectronic applications especially in solar cells as window layers.

(Received July 9, 2017; Accepted August 29, 2017)

Keywords: Bandgap, Transmittance, Chemical bath, Optical density, Zinc sulphide, Annealing, Concentration

1. Introduction

Zinc sulphide a group II –VI semiconductor has been widely reported. Zinc sulphide (ZnS) has a wide direct bandgap in the near UV regions of the spectrum. This wide bandgap possessed by Zinc sulphide makes it good candidate [1] in many applications such as fabrication of optoelectronic devices, electroluminescent devices, optical coatings etc. It is also an important material in the design of antireflection coatings and in the detection and modulation of visible and near ultra violet light [2]. The use of ZnS thin films multilayer dielectric filters had also been reported. Many methods have been used to deposit ZnS thin films. Such method like molecular beam epitaxy, multi –organic chemical vapour deposition, chemical bath deposition technique etc, had been previously reported [3, 4]. A lot of techniques can be used to modify the energy bandgap of materials. Deposition parameters like deposition time, deposition temperature, concentration of precursors, post depositing annealing to mention but few are some of the parameters that affect the band gap of materials. Any of these parameters can affect the size distribution, quantum size effect can be altered. For instance, increase in substrate temperature has been found to cause a reduction in the bandgap which is due to [4, 5] the reorganization of the atoms arising from the evaporation of water molecule. The addition of impurities (doping) has also been reported to have significant effect on the band gap of materials. Doping helps to change the fluctuation in the d-space and position which creates a non-linear band gap and this defines the optical and electrical behaviour of materials [6]. In the present research, we investigated the effect of varying concentration and post deposition annealing on the optical properties of ZnS thin films deposited using the chemical

*Corresponding author: patricknwofe@gmail.com

bath technique with emphasis on tailoring the band gap of the material for enhanced device applications.

2. Experimental

Substrate cleaning plays a vital role in obtaining uniform films that are free from pin-holes in thin film deposition independent of the deposition technique. In this study, the soda lime glass slide that were used as substrates were thoroughly cleaned hence prior to the deposition, the glass slides were immersed in concentrated trioxonitrate (V) acid (HNO_3) for 48 hours and finally rinsed in distilled water and dried in an oven before using them as the substrates. Each of the chemical bath for the deposition of the ZnS thin films consists of 15 ml of 0.1 M, 0.3M and 0.5 M of $ZnCl_2$, 0.3 M of Thiorea, 0.3 M of citric acid and 4 ml of ammonia respectively. In each case four glass slides (substrate) were inserted vertically through a synthetic foam into the bath and the whole arrangement was immersed in a water bath maintained at a temperature of 65 ^{0}C. Deposition was allowed to take place for 2 hours. Thereafter the coated glass slides were removed, washed in running water and rinsed with distilled water and dried in the air. The films were subjected to post-deposition heat treatment with annealing temperatures in the range 100 ^{o}C to 200 ^{o}C, with the annealing time fixed for 1 hour. The films were characterized using optical spectroscopy to investigate the transmittance and reflectance versus wavelength measurements. A Unico –UV-2102 PC spectrophotometer operated at normal incident of light in the wavelength range of 280 nm to 1000 nm was used for the investigation and all the transmittance and reflectance versus wavelength measurements were done at room temperature of 298 K.

3. Results and discussion

Fig. 1 gives the transmittance versus wavelength λ spectra for the as-deposited layers while Fig. 2 indicates the transmittance versus wavelength λ plots for the layer annealed at 100 ^{o}C for 1 hour.

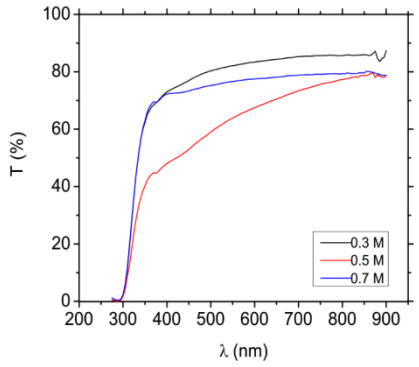

Fig. 1. Transmittance vs λ for as-deposited films

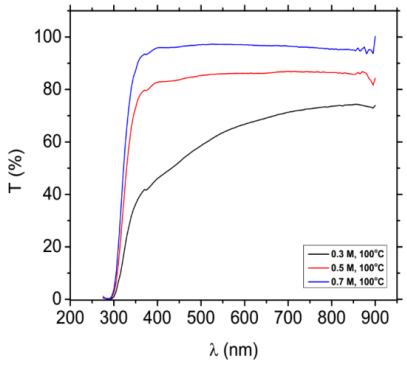

Fig. 2. Transmittance vs λ of films annealed at 100^o C

As indicated in the experimental section, the optical properties of the films deposited on a glass substrate were determined from the transmission and reflectance spectra in the range of 280 – 1000 nm. The transmission spectra of the deposited films at different $Zn^{2+}$and post deposition annealing at different temperatures of 150 ^{o}C and 200 ^{o}C are shown in Figures 3 to 4 respectively. In Fig.1 it is observed that the film deposited with 0.3m of Zn^{2+} has the highest value of transmittance of about 80% followed by film deposited with 0.7M of Zn^{2+} while the film deposited with 0.5 M of Zn^{2+} recorded the lowest value of transmittance. In figures 2 to 3, the transmittance curve shows that the transmittance of the films were modified by post deposition annealing. As depicted in the curves, it is evident that as the annealing temperature increases, the transmittance

decreases irrespective of the concentration of the principal precursor and is optimum at 150 ^{o}C. Generally from the plots of transmittance versus wavelength for the thin films under study (Figs.3 and 4), it is observed that the transmittance is high in the visible and near infra-red region and minimum at wavelength approximately 300 nm. The increase in transmittance may be attributed to the transition of ZnS from amorphous to polycrystalline structure as annealing temperature increases. A relative high transmittance of the films as annealing temperature increases may be linked to scattering due to the decrease in the grain size distribution. Similar findings have been reported by other authors [7, 8].

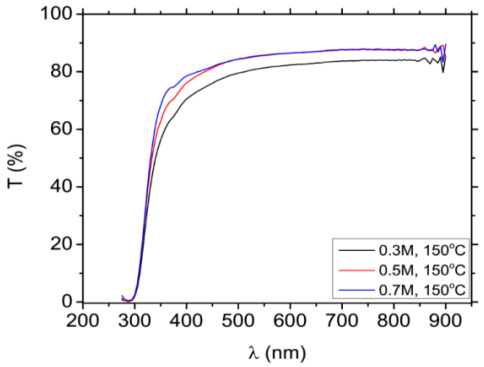

Fig. 3. Transmittance vs λ of films annealed at 150^{o} C

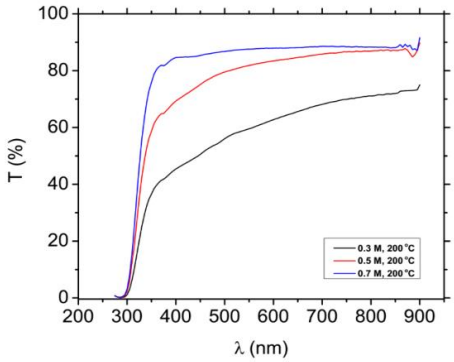

Fig. 4. Transmittance vs λ films annealed at 200^{o} C

The variation of extinction coefficient against photon energy (hν) is shown in Figs 5 to 8. It is observed that before the absorption edge, the variation of k with photon energy is constant. However, immediately after the absorption edge, k increases with increase in photon energy. The variation of k with photon energy with variation in Zn^{2+} and annealing temperature is shown in Tables 1, 2 and 3.

Table 1. Variation of k and E_g with 0.3 M Zn^{2+} concentration and post deposition temperature

Conc. (M)	Post Deposition temperature ^{o} C	k	E_g(eV)
0.3	-	0.5	3.73
0.3	100	0.4	3.48
0.3	150	0.47	3.62
0.3	200	0.35	3.64

Table 2: Variation of k and E_g with 0.5 M Zn^{2+} concentration and post deposition temperature

Conc. (M)	Post Deposition temperature ^{o} C	k	E_g(eV)
0.5	-	0.51	3.48
0.5	100	0.48	3.61
0.5	150	0.53	3.72
0.5	200	0.45	3.66

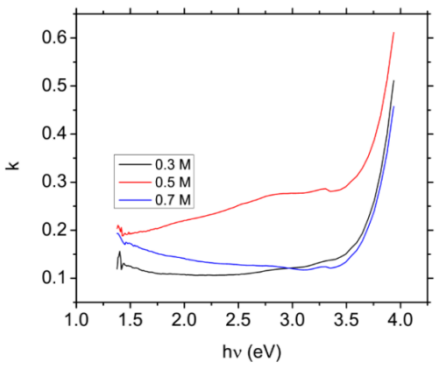

Fig.5: Plot of K vs hν for as-deposited films

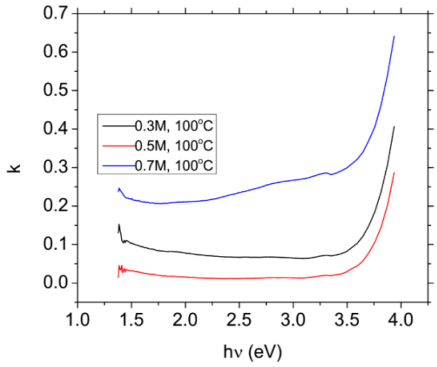

Fig.6. Plot of K vs for films annealed at 100^o C

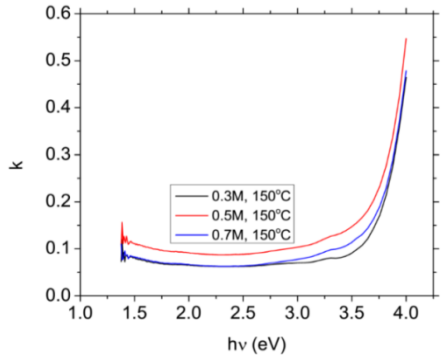

. Fig.7: Plot of K vs hν for films annealed at 150 ^{o}C

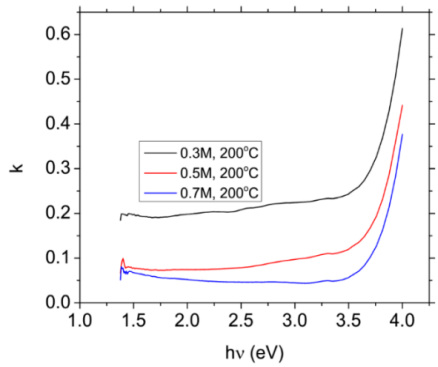

Fig.8: Plot of K vs hν for films annealed at 200 ^{o}C

Figs. 9 – 12 show the plots for the determination of the energy bandgap. The energy bandgaps were obtained by extrapolating the straight portions of the $((\alpha h\nu)^2$ versus $h\nu$ to zero absorption coefficients. The bandgaps were deduced using relevant equations from the literature [9] to obtain the optical absorption coefficient α and hence the energy bandgap Eg. Thus the optical absorption coefficient α was deduced using the equation [9, 10];

$$\alpha = \frac{1}{d}\ln\left(\frac{100}{T\,\%}\right) \tag{1}$$

In equation 1, α retains its meanings, d is the film thickness and T is the transmittance in percentage. The energy bandgap was determined using the equation [11,12];

$$(\alpha h\nu) = B\left(h\nu - E_g\right)^n \tag{2}$$

Where α retains its meaning, h is the Planck's constant, ν is the frequency of the electromagnetic radiation, B is an energy independent constant, but generally depend on the refractive index and the effective masses of the hole and electron respectively as contained in the literature [12, 13], Eg is the energy bandgap, and n is an index that characterise the nature of the transition exhibited by the materials under study. In direct transition, it is generally accepted that n = 1/2. The determined bandgaps are as listed in Tables 1 to 2. It is evident from the Tables and Figures that the bandgap increases with increase in annealing temperature especially when the concentration of the Zn^{2+} is 0.7M. However, the range of bandgaps for the different concentration of Zn^{2+} and at different post deposition temperature are 3.73 eV - 3.64 eV, 3.5 eV – 3.76 eV and 3.74 eV – 3.76 eV for 0.3 M,

0.5M and 0.7 M of Zn^{2+} respectively. These values of bandgap are indicated in Table 3 and the values are in close agreement with recent reports in the literature [14, 15, 16]. The slight decrease in the bandgap as the annealing temperature increases can be attributed to quantum size effect of the ZnS thin films [6, 8, 15, 17, 18]. It is also evident from the results that increasing the concentration of the principal precursor increases the band gap.

Table 3. Variation of k and E_g with 0.7 M Zn^{2+} concentration and post deposition temperature

Conc. (M)	Post Deposition temperature ^{o} C	k	E_g(eV)
0.7	-	0.60	3.59
0.7	100	0.55	3.71
0.7	150	0.55	3.74
0.7	200	0.45	3.76

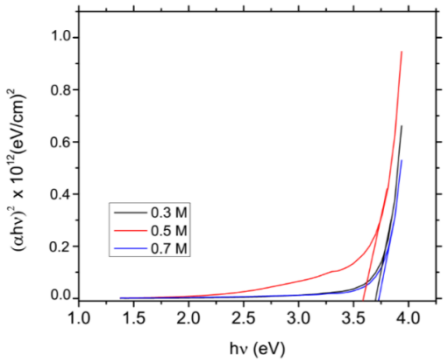

Fig.9: Plot for determination of bandgap for as-deposited films

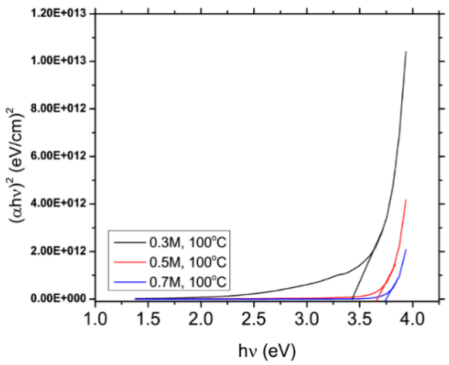

Fig.10: Plot for determination of bandgap for films annealed at 100^{o} C

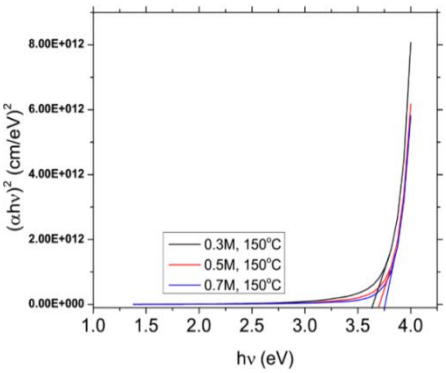

Fig.11. Plot for determination of bandgap for films annealed at 150^{o} C

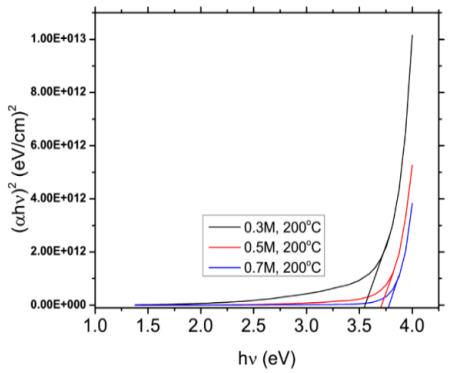

Fig.12: Plot for determination of bandgap for films annealed at 200^{o} C

The plot of optical density against photon energy is shown in Figs 12 – 16 for the as-grown and annealed layer respectively. The plots indicates that for all the samples, the optical density increased almost linearly with increasing photon energy up to the absorption edge after which a sharp rise in optical energy was noticed except for the film composition having 0.5 M of Zn^{2+} and annealed at 150^{o} C. These behavior implies good transparency beyond the bandgap of the films irrespective of the concentration of zinc ions and the post deposition annealing temperature. The variation of the optical density with varying post deposition annealing temperature can also be linked in terms of the stoichiometric changes induced by sulphide vacancies and neutral defects. The formation of these defects depends on the sticking coefficient, nucleation rates and the

migration of impinging zinc and sulphide ions during deposition which is a function of the concentration of the reacting species. Other authors have reported similar findings in the literature [16, 19, 20].

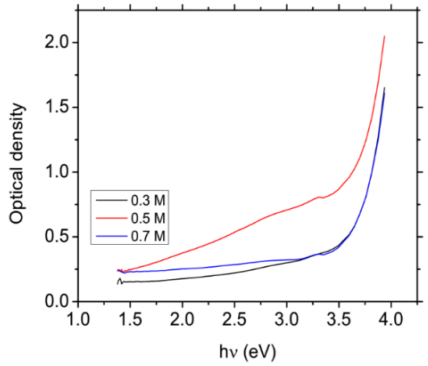

Fig. 13: Plot of Optical density vs hν for as-deposited films

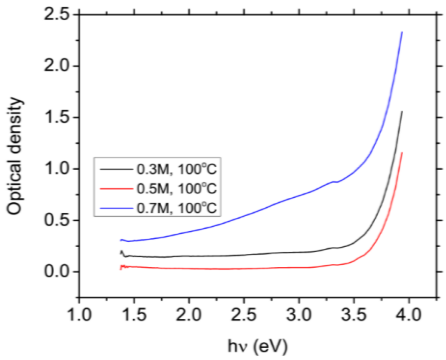

Fig. 14: Plot of Optical density vs hν for films annealed at 100^o C

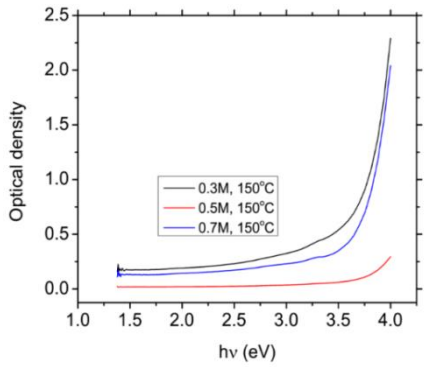

Fig. 15. Plot of Optical density vs hν for films annealed at 150^o C

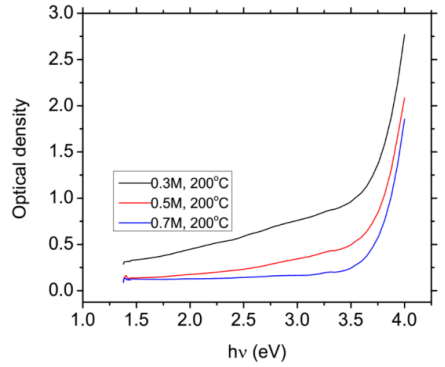

Fig. 16. Plot of Optical density vs hν for films annealed at 200^{o}C

4. Conclusions

The effect of varying concentration and post deposition annealing as a means of further tailoring the bandgap of ZnS thin films prepared by the chemical bath method is reported. The effects of these parameters on some optical properties of the films is also reported, The results of the investigations shows that the bandgap of the deposited ZnS thin films were direct and ranges from 3.5 eV to 3.76 eV.

References

[1] D. Hwang, C.S. Son, Journal of Nanoscience and Nanotechnology, **17** (7), 5042 (2017).
[2] K. Nabesaka, Y. Ishikawa, Y. Hosokawa, Y. Uraoka, Applied Physics Express **10**(2), 021201 (2017).
[3] A. Q. Meng, X. Xiong, K. Qiu, Y. Lin, Nanotechnology **28**(10), 105502 (2017).
[4] H. Abdullah, N. Abrusheed, S. Shaari, World Applied Sciences Journal **9**(8), 1087 (2012).
[5] D.A. Johnson, M.H. Corletto, K.T. Reddy, I. Forbes, R.W. Miles, Thin Solid Films **1,** 403 (2002).
[6] G. Nabiyouni, R Sahraei, M. toghiany, M. majies Ara, K. Hadayati, Rev. Adv. Mater.

Sc. **27**, 62 (2011).
[7] P.E. Agbo. P.A. Nwofe, C. A. Elekwa, Journal of Ovonic Research, **12** (3), 163 (2016).
[8] W. Rika, H. Hardhienata, IOP Conference Series: Earth and Environmental Science, **54**(1), 012094 (2017).
[9] P.E. Agbo, P.A. Nwofe, M.N. Ede, Journal of non- Oxide glasses, **8**(4), 85 (2016)
[10] P.A. Nwofe, P.E. Agbo, J. Non-Oxide Glasses, **9(**1), 9 (2017)
[11] B. Ismail, S. Mushtaq, A. Khan, Chalcogenide Letters. **11**(1), 37 (2014).
[12] J.I. Pankove, Optical Processes in Semiconductors, Prentice-Hall, Englewood Cliffs, New Jersey, 1971.
[13] M. Sreedhar, I. Neelakanta Reddy, P. Bera, T. S. Shyju, C. Anandan, Surface and Interface Analysis **49**(4), 284 (2017).
[14] D.U. Onah, P.A. Nwofe, H.E. Uguru, Research Journal of Applied Sciences, Engineering and Technology **13**(3), 253 (2016).
[15] K. Petkov,R. Todorov, D. Kozhuharova, I.Tcky, E. Cernoskova, P.J.S.Ewen, J. Mat. Sci. **39(**961), (2006)
[16] P.E. Agbo, Adv. Appl. Sci. Res, **2**(6), 393 (2011).
[17] P.A. Nwofe, K.T.R. Reddy, R.W. Miles, Advanced Materials Research **602**, 1409 (2013).
[18] P.A. Nwofe, K.T.R. Reddy, R.W. Miles, IEEE 39th Photovoltaic Specialists Conference (PVSC), **14115963**, 2518 (2013).
[19] P.A. Nwofe, J. Nano. Adv. Mat. **3**(2), 115 (2015).
[20] L. Kong, J. Deng, L. Chen, Chalcogenides Letts., **14**(3), 87 (2017).